Inorg. Chem. **2006**, *45*, 10224–10229

Inorganic Chemistry Article

Magnetic Properties of $BiMnO_3$ Studied with Dc and Ac Magnetization and Specific Heat

Alexei A. Belik* and Eiji Takayama-Muromachi

Advanced Nano Materials Laboratory (ANML), National Institute for Materials Science (NIMS), 1-1 Namiki, Tsukuba, Ibaraki 305-0044, Japan

Received July 26, 2006

Magnetic and specific heat measurements were performed in a single-phased powder $BiMnO_3$ sample prepared at 6 GPa and 1383 K. The imaginary part of the ac susceptibilities showed strong frequency dependence below the ferromagnetic Curie temperature of 98 K. The relaxation measurements revealed time-dependent magnetic properties below 98 K. These data indicate the appearance of a "spin-glass-like" state in $BiMnO_3$. Specific heat measurements showed the existence of ferromagnetic spin waves. However, no simple term $C_m \propto T^{3/2}$ was found indicating an unconventional behavior of the magnetic specific heat. The Debye temperature was estimated to be 410 K using isostructural compounds $BiScO_3$ and $BiCrO_3$.

Introduction

Multiferroic materials have received renewal interest in recent years.[1−3] In multiferroic systems, two or all three of (anti)ferroelectricity, (anti)ferromagnetism, and ferroelasticity are observed in the same phase.[4] Such systems are rare in nature but potentially studied with interest in wide technological applications.[1−3]

$BiMnO_3$ has been extensively studied as a multiferroic material.[5−25] Thin film samples of $BiMnO_3$ showed promising results for practical applications.[13−18] $BiMnO_3$ is a well-established ferromagnet below $T_M = 99-103$ K.[6,9,11,19,20] It is believed to crystallize in monoclinic space group $C2$ at room temperature (RT) with lattice parameters of $a = 9.5323$ Å, $b = 5.6064$ Å, $c = 9.8535$ Å, and $\beta = 110.667°$.[7] $BiMnO_3$ undergoes two high-temperature phase transitions at 470 and 770 K.[6,11,19−21] The phase transition at 470 K is monoclinic-to-monoclinic phase transition without any detectable change in the symmetry.[11,21] The phase transition at 770 K is monoclinic-to-orthorhombic.[11] Below T_M, the three-dimensional (3D) magnetic structure is realized with the magnetic moments of Mn^{3+} parallel to the b axis.[9] No change of the

* To whom correspondence should be addressed. E-mail: Alexei.BELIK@nims.go.jp.

(1) (a) Eerenstein, W.; Mathur, N. D.; Scott, J. F. *Nature (London)* **2006**, *442*, 759. (b) Khomskii, D. I. *J. Magn. Magn. Mater*. **2006**, *306*, 1.
(2) Fiebig, M. *J. Phys. D: Appl. Phys.* **2005**, *38*, R123.
(3) Hill, N. A. *Annu. Rev. Mater. Res.* **2002**, *32*, 1.
(4) Hill, N. A. *J. Phys. Chem. B* **2000**, *104*, 6694.
(5) Tomashpol'skii, Y. Y.; Zubova, E. V.; Burdina, K. P.; Venevtsev, Y. N. *Inorg. Mater.* **1967**, *3*, 1861.
(6) Sugawara, F.; Iiida, S.; Syono, Y.; Akimoto, S. *J. Phys. Soc. Jpn.* **1968**, *25*, 1553.
(7) Atou, T.; Chiba, H.; Ohoyama, K.; Yamaguchi, Y.; Syono, Y. *J. Solid State Chem.* **1999**, *145*, 639.
(8) Seshadri, R.; Hill, N. A. *Chem. Mater.* **2001**, *13*, 2892.
(9) Moreira dos Santos, A.; Cheetham, A. K.; Atou, T.; Syono, Y.; Yamaguchi, Y.; Ohoyama, K.; Chiba, H.; Rao, C. N. R. *Phys. Rev. B* **2002**, *66*, 064425.
(10) dos Santos, A. M.; Parashar, S.; Raju, A. R.; Zhao, Y. S.; Cheetham, A. K.; Rao, C. N. R. *Solid State Commun.* **2002**, *122*, 49.
(11) Kimura, T.; Kawamoto, S.; Yamada, I.; Azuma, M.; Takano, M.; Tokura, Y. *Phys. Rev. B* **2003**, *67*, 180401(R).
(12) Shishidou, T.; Mikamo, N.; Uratani, Y.; Ishii, F.; Oguchi, T. *J. Phys.: Condens. Matter* **2004**, *16*, S5677.
(13) Sharan, A.; An, I.; Chen, C.; Collins, R. W.; Lettieri, J.; Jia, Y. F.; Schlom, D. G.; Gopalan, V. *Appl. Phys. Lett.* **2003**, *83*, 5169.
(14) Sharan, A.; Lettieri, J.; Jia, Y.; Tian, W.; Pan, X.; Schlom, D. G.; Gopalan, V. *Phys. Rev. B* **2004**, *69*, 214109.
(15) dos Santos, A. F. M.; Cheetham, A. K.; Tian, W.; Pan, X. Q.; Jia, Y. F.; Murphy, N. J.; Lettieri, J.; Schlom, D. G. *Appl. Phys. Lett.* **2004**, *84*, 91.
(16) Son, J. Y.; Kim, B. G.; Kim, C. H.; Cho, J. H. *Appl. Phys. Lett.* **2004**, *84*, 4971.
(17) Gajek, M.; Bibes, M.; Barthelemy, A.; Bouzehouane, K.; Fusil, S.; Varela, M.; Fontcuberta, J.; Fert, A. *Phys. Rev. B* **2005**, *72*, 020406.
(18) Eerenstein, W.; Morrison, F. D.; Scott, J. F.; Mathur, N. D. *Appl. Phys. Lett.* **2005**, *87*, 101906.
(19) Chi, Z. H.; Xiao, C. J.; Feng, S. M.; Li, F. Y.; Jin, C. Q.; Wang, X. H.; Chen, R. Z.; Li, L. T. *J. Appl. Phys.* **2005**, *98*, 103519.
(20) Montanari, E.; Righi, L.; Calestani, G.; Migliori, A.; Gilioli, E.; Bolzoni, F. *Chem. Mater.* **2005**, *17*, 1765.
(21) Montanari, E.; Calestani, G.; Migliori, A.; Dapiaggi, M.; Bolzoni, F.; Cabassi, R.; Gilioli, E. *Chem. Mater.* **2005**, *17*, 6457.
(22) Yang, H.; Chi, Z. H.; Li, F. Y.; Jin, C. Q.; Yu, R. C. *Phys. Rev. B* **2006**, *73*, 024114.
(23) Chi, Z.; Yang, H.; Li, F.; Yu, R.; Jin, C.; Wang, X.; Deng, X.; Li, L. *J. Phys.: Condens. Matter* **2006**, *18*, 4371.
(24) Yang, C. H.; Koo, T. Y.; Lee, S. H.; Song, C.; Lee, K. B.; Jeong, Y. H. *Europhys. Lett.* **2006**, *74*, 348.
(25) Yang, C. H.; Koo, J.; Song, C.; Koo, T. Y.; Lee, K. B.; Jeong, Y. H. *Phys. Rev. B* **2006**, *73*, 224112.

10.1021/ic061400b CCC: $33.50

Published on Web 11/09/2006

crystal symmetry was found below T_M. Despite a large number of works, the low-temperature magnetic properties of $BiMnO_3$ have been investigated poorly. Note that $BiMnO_3$ is a rare example of an insulating ferromagnet,[11] and a spin-wave contribution to magnetic properties is expected.

It was found recently that the structure of $BiScO_3$ is very close to that of $BiMnO_3$, but $BiScO_3$ crystallizes in the centrosymmetric space group *C*2/*c*.[26] Because there is no magnetic ions in $BiScO_3$, it can be used to estimate the lattice contribution in the specific heat. $BiCrO_3$ was reported to be isostructural with $BiMnO_3$.[27]

To achieve a better understanding of the properties of $BiMnO_3$ at low temperatures we have performed dc/ac magnetic and specific heat measurements on single-phased powder samples. These measurements revealed the existence of "spin-glass-like" features, spin waves, and unconventional behavior of the magnetic specific heat.

Experimental Section

A mixture of Bi_2O_3 (99.99%) and Mn_2O_3 with an amount-of-substance ratio of 1:1 was placed in Au capsules and treated at 6 GPa in a belt-type high-pressure apparatus at 1383 K for 60−70 min. After heat treatment, the samples were quenched to RT, and the pressure was slowly released. The resultant samples were black powder. X-ray powder diffraction (XRD) showed that the samples were single phased. Single-phased Mn_2O_3 was prepared from a commercial MnO_2 (99.99%) by heating in air at 923 K for 24 h. Single-phased $BiScO_3$ was prepared from Bi_2O_3 and Sc_2O_3 (99.9%) at 6 GPa and 1413 K for 40 min,[26] and single-phased $BiCrO_3$, from Bi_2O_3 and Cr_2O_3 (99.9%) at 6 GPa and 1653 K for 120 min.[27] $BiScO_3$ was white powder, and $BiCrO_3$ was a khaki-green dense pellet.

Magnetic susceptibilities, $\chi = \mathbf{M}/\mathbf{H}$, of $BiMnO_3$ were measured on a SQUID magnetometer (Quantum Design, MPMS) between 2 and 350 K in applied fields of 5×10^{-4} and 1 T (1 T = $(10^7/4\pi)$ A m^{-1}) under both zero-field-cooled (ZFC) and field-cooled (FC) conditions. Isothermal magnetization measurements were performed between −7 and 7 T at 5 K. Frequency dependent ac susceptibility measurements at zero static magnetic field were performed with a Quantum Design PPMS instrument from 200 to 2 K at frequencies (*f*) of 10, 10^2, 5×10^2, 10^3, 5×10^3, and 10^4 Hz and an applied oscillating magnetic field (H_{ac}) of 5×10^{-4} T. Specific heat, C_p, of $BiMnO_3$, $BiCrO_3$, and $BiScO_3$ at zero static magnetic field was recorded between 2 and 300 K on cooling by a pulse relaxation method using a commercial calorimeter (Quantum Design PPMS). The C_p vs T curves of $BiMnO_3$ were also recorded at 0 and 9 T on heating from 2 to 300 K and on cooling from 10 to 0.4 K. No difference was found between the C_p vs T curves of $BiMnO_3$ measured on cooling and heating at 0 T. For the specific heat measurements, the powder samples of $BiMnO_3$ and $BiScO_3$ were cold-pressed at 1 GPa to make pellets. The thermoremanent magnetization (TRM) curve was measured at zero magnetic field on heating after cooling the sample from 150 to 2 K at 0.1 T. The time-dependent relaxation curves were measured in two modes: (1) at zero magnetic field after cooling the sample from 150 K to the desired temperature at 0.1 T (the magnetic field was set to zero after 5 min after reaching the desired temperature); (2) at 10^{-3} T after cooling the sample from 150 K to the desired temperature at zero magnetic field.

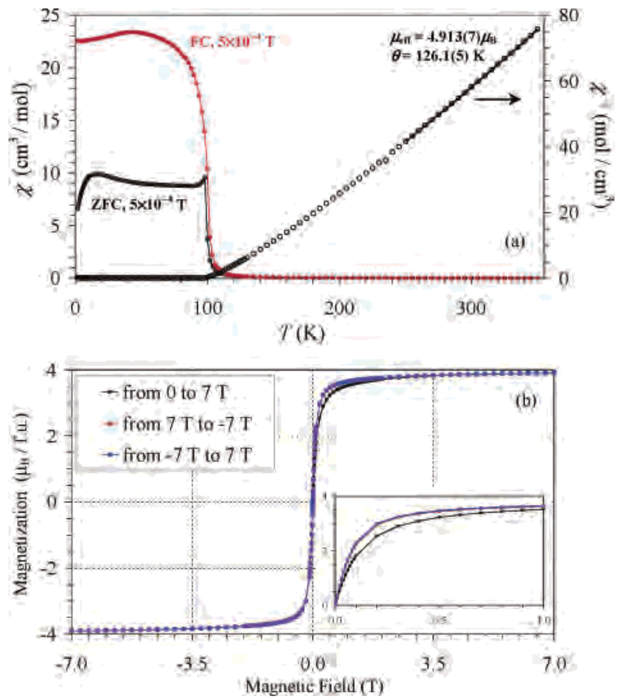

Figure 1. (a) ZFC and FC dc magnetic susceptibility ($\chi = \mathbf{M}/\mathbf{H}$) curves of $BiMnO_3$ measured at 5×10^{-4} T. The secondary axis gives the inverse ZFC curve (circles) with the Curie−Weiss fit (line). (b) Isothermal magnetization curves at 5 K. The inset shows the curves between 0 and 1 T.

Results and Discussion

Figure 1a shows magnetic susceptibilities of $BiMnO_3$ between 2 and 350 K. The transition to the ferromagnetic state in $BiMnO_3$ is observed at $T_M = 98$ K as determined by the peak on the ZFC $d(\chi T)/dT$ vs T curve. A very small anomaly is also observed near 114 K. The similar anomaly was reported in the literature and explained by the presence of a small amount of another perovskite-like modification of $BiMnO_3$.[20] This modification was detected by electron diffraction. Note that it cannot be detected by powder diffraction methods because its reflections overlap with the reflections of the main monoclinic phase. A pronounced irreversibility is observed between the ZFC and FC curves measured at 5×10^{-4} T. This irreversibility starts just below T_M. On the other hand, the ZFC and FC curves almost coincide with each other when measured at 1 T. The inverse ZFC magnetic susceptibilities between 250 and 350 K are fit by the modified Curie−Weiss equation

$$\chi(T) = \chi_0 + \mu^2_{\text{eff}} N(3k_B(T - \Theta))^{-1} \quad (1)$$

where χ_0 (=$-2.0(3) \times 10^{-4}$ cm^3/mol) is the temperature-independent term, μ_{eff} (=4.913(7) μ_B) is effective magnetic moment, N is Avogadro's number, k_B is Boltzmann's constant, and Θ (=126.1(5) K) is the Weiss constant. The effective magnetic moment is close to the localized Mn^{3+} moment of 4.90 μ_B.

(26) Belik, A. A.; Iikubo, S.; Kodama, K.; Igawa, N.; Shamoto, S.; Maie, M.; Nagai, T.; Matsui, Y.; Stefanovich, S. Yu.; Lazoryak, B. I.; Takayama-Muromachi, E. *J. Am. Chem. Soc.* **2006**, *128*, 706.
(27) Niitaka, S.; Azuma, M.; Takano, M.; Nishibori, E.; Takata, M.; Sakata, M. *Solid State Ionics* **2004**, *172*, 557.

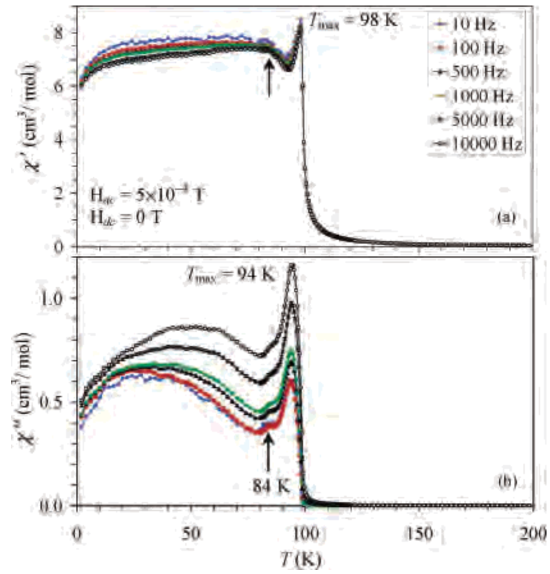

Figure 2. (a) Real χ' and (b) imaginary χ'' parts of the ac susceptibility as a function of temperature (at 2−200 K) at frequencies $f = 10$, 100, 5×10^2, 10^3, 5×10^3, and 10^4 Hz for $BiMnO_3$. Measurements were performed on cooling at zero static field using an ac field with the amplitude $H_{ac} = 5 \times 10^{-4}$ T. The positions of maxima are given. The arrows show additional anomalies.

Figure 1b depicts the isothermal magnetization curves at 5 K. A very small hysteresis is observed with the coercive field (H_c) of about 3×10^{-4} T and the remnant magnetization (M_r) of about 1.3×10^{-2} μ_B/Mn^{3+} ion. These values are much smaller than the previously reported ones, e.g., $H_c = 0.02$ T and $M_r = 0.2$ μ_B.[19,23] The magnetic moment at 5 K and 7 T was about 3.9 μ_B. This value is very close to the fully aligned spin value of 4 μ_B for Mn^{3+} and the largest among the previously reported ones of about 3.6 μ_B.[11] Note that the first magnetization curve from 0 to 7 T is slightly different from other curves (the inset of Figure 1b). This behavior of magnetization curves was observed in other manganites exhibiting spin-glass-like features.[28]

Figure 2 shows the ac susceptibility curves of $BiMnO_3$. Sharp peaks are observed at 98 K on the χ' vs T curve, while the χ'' vs T curves exhibit peaks at 94 K. The first point to note is that the imaginary parts are still observed below T_M down to 2 K. In a conventional ferromagnet, the imaginary part should have a peak at T_M and vanish above and below T_M. The peak positions are almost frequency independent. However the peak intensity of χ'' vs T is strongly increased with increasing frequency, while the peak intensity of χ' vs T almost does not change. The second point to note is the observation of additional anomalies at 84 K on both χ' vs T and χ'' vs T curves, whose origin is not clear now, and very broad frequency-dependent features below 80 K on the χ'' vs T curves. The peaks near T_M on both χ' vs T and χ'' vs T curves signal the onset of a ferromagnetic order, whereas frequency-dependent anomalies below T_M are associated with "spin-glass-like" states. It should be noted that no anomaly is found near 114 K, where the anomaly is observed on the dc susceptibilities. Above 120 K, the ac and dc susceptibility curves coincide with each other.

Therefore, the ac susceptibility measurements reveal the spin-glass-like anomalies in $BiMnO_3$ below T_M. There are two possible explanations for the observed spin-glass features. The first explanation is the existence of peculiar orbital order[25] and ferromagnetic- and antiferromagnetic-type interactions between Mn^{3+} ions derived from the direction of the Jahn−Teller distortion.[7,9,24,25] On the other hand, in the magnetically ordered state below T_M, all the moments are aligned ferromagnetically.[9] These facts produce magnetic frustration. It is known that the competition between ferromagnetic- and antiferromagnetic-type interactions is necessary to produce a spin-glass state. The second explanation is possible tiny changes of the stoichiometry of $BiMnO_3$. For example, spin-glass-like states were observed in $LaMnO_{3+\delta}$ with $\delta > 0$.[29] The stoichiometry changes may also explain the differences in H_c and M_r between our samples and the literature data.[19,23] Note that, in ref 30, spin-glass-like features observed in $La_{1-x}MnO_3$ were explained by the domain wall pinning effects. The origin of the pinning effects was proposed to be a nonuniform distribution of rather large amount of Mn^{4+} ions or mild structural distortions at lower temperatures. However, this is not the case in $BiMnO_3$. In addition, there are differences in the ac susceptibility and relaxation curves (see below) between $BiMnO_3$ and $La_{1-x}MnO_3$.

The TRM curve (see the experimental part for the definition) as a function of temperature is given in Figure 3a. After a noticeable decrease of the TRM from 2 to about 12 K, there is a plateaulike region. Then, the TRM gradually decreases when approaching T_M. The logarithmic presentation clearly demonstrates the presence of a ferromagnetic contribution below 114 K in consistence with the dc susceptibilities. Figure 3b depicts the time-dependent relaxation curves measured at 10^{-3} T. The slowest relaxation is observed at the intermediate temperatures of 50−80 K. The relaxation is hastened on increasing or decreasing temperature. The similar behavior is found when the relaxation was measured at zero magnetic field after cooling in a magnetic field of 0.1 T. The relaxation almost follows the logarithmic law below 80 K. The deviation from the logarithmic dependence is observed when approaching T_M (at 90 and 95 K). The TRM curve is in consistence with the relaxation measurements, that is, the decrease of the magnetization with temperature is fast at very low temperatures and near T_M that suggests the faster time-dependent relaxation at these temperature ranges. $BiMnO_3$ clearly shows the time-dependent magnetic properties. This behavior was recently observed in thin-film samples of $BiMnO_3$ and explained by in-plane compressive strains in the film.[24] Our results indicate that the magnetic frustration and spin-glass-like magnetic properties are intrinsic to $BiMnO_3$ independent of the bulk or thin-film forms.

(28) Karmakar, S.; Taran, S.; Chaudhuri, B. K.; Sakata, H.; Sun, C. P.; Huang, C. L.; Yang, H. D. *Phys. Rev. B* **2006**, *74*, 104407 and references therein.

(29) Ghivelder L.; Castillo, I. A.; Gusmao, M. A.; Alonso, J. A.; Cohen, L. F. *Phys. Rev. B* **1999**, *60*, 12184.

(30) Sankar, C. R.; Joy, P. A. *Phys. Rev. B* **2005**, *72*, 024405.

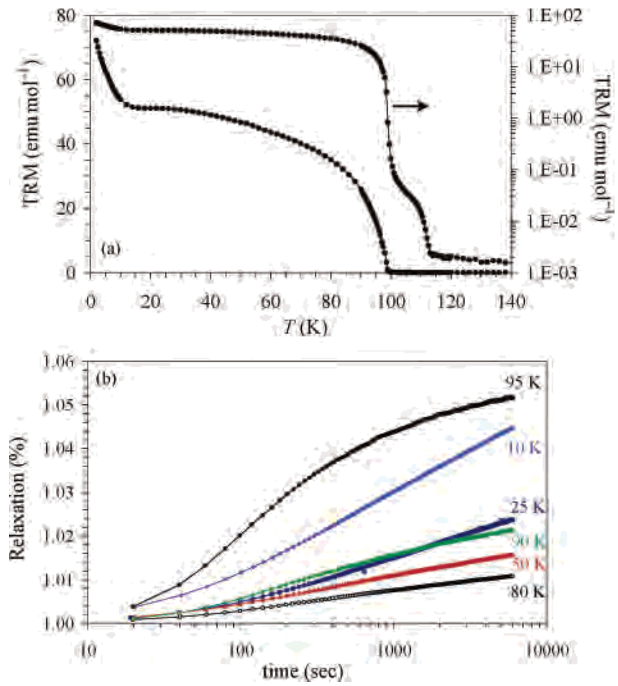

Figure 3. (a) Thermoremanent magnetization (TRM) curve as a function of temperature for $BiMnO_3$. The TRM curve was measured at zero magnetic field on heating after cooling the sample from 150 to 2 K at 0.1 T. The secondary *y* axis gives the same curve in the logarithmic scale. (b) Relative change of magnetization in % as a function of time (relaxation). The curves were measured at 10^{-3} T after cooling the sample from 150 K to the desired temperature at zero magnetic field.

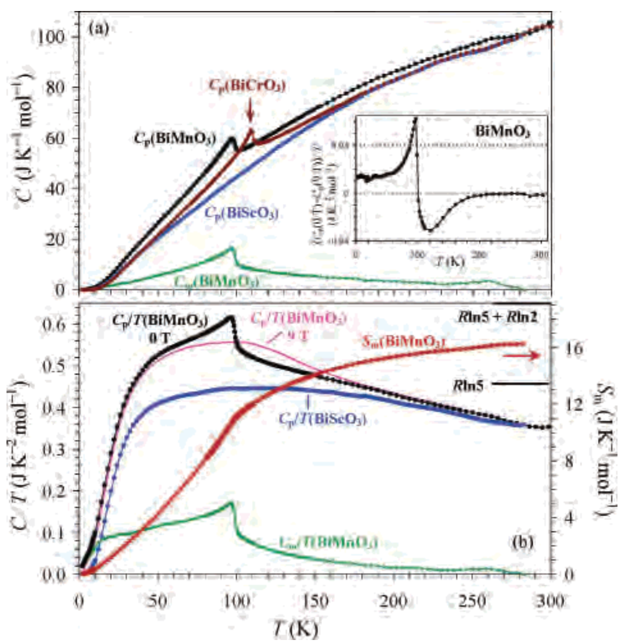

Figure 4. (a) *C* vs *T* curves between 2 and 300 K for $BiMnO_3$ (C_p and C_m), $BiCrO_3$ (C_p), and $BiScO_3$ (C_p) at zero magnetic field. The magnetic specific heat (C_m) was obtained by subtracting the total specific heat of $BiScO_3$ from that of $BiMnO_3$. The inset gives the $(C_p(0\ T) - C_p(9\ T))/T$ vs *T* curve of $BiMnO_3$. (b) *C*/*T* vs *T* curves between 2 and 300 K for $BiMnO_3$ (C_p at 0 and 9 T and C_m at 0 T) and $BiScO_3$ (C_p). The secondary axis shows the temperature dependence of the magnetic entropy S_m in $BiMnO_3$.

Figure 4 shows the specific heat of $BiMnO_3$ plotted as C_p vs *T* and C_p/T vs *T* in the temperature range of 2 and 300 K. The λ-type anomaly on the C_p vs *T* is observed with the maximum at 97.5 K in agreement with the previous measurements.[11] The lattice contribution (C_l) in $BiMnO_3$ is estimated using $BiScO_3$ containing no magnetic ions.[26] We also measured the C_p vs *T* curve of another isostructural compound, $BiCrO_3$, that orders antiferromagnetically at $T_N = 114$ K.[6,27] In the temperature ranges of 2−50 and 180−300 K, the C_p vs *T* curves of $BiCrO_3$ and $BiScO_3$ are very similar to each other (Figure 4a) indicating that $BiScO_3$ can give good approximation to the C_l. The magnetic specific heat (C_m) of $BiMnO_3$ is obtained by subtracting the total specific heat of $BiScO_3$ from that of $BiMnO_3$. The estimated magnetic entropy

$$S_m = \int (C_m/T)\, dT \qquad (2)$$

is about 16.3 J K^{-1} mol^{-1} at 280 K (Figure 4b). This value is larger than the spin-only value of $R \ln(2S + 1) = R \ln 5 = 13.4$ J K^{-1} mol^{-1} expected for the $S = 2$ systems (*S* is spin). The expected value is reached near 135 K. It may be explained by difficulties in accurate measurements of C_p at high temperatures and also by the fact that there is a strong Jahn−Teller distortion in $BiMnO_3$ compared with $BiScO_3$ and $BiCrO_3$. The distortion in $BiMnO_3$ may have an effect on the lattice specific heat. However, if we take into account that $BiMnO_3$ undergoes orbital ordering at a certain temperature,[25] the minimum entropy change over a wide temperature range should be $R \ln 5 + R \ln 2 = 19.1$ J K^{-1} mol^{-1}. There is a large part of the magnetic specific heat above T_M in $BiMnO_3$ and also above T_N in $BiCrO_3$ (Figure 4a) probably due to the short-range correlations.

The specific heat is analyzed in more detail below 10 K. Figure 5 depicts the *C*/*T* vs *T* and *C*/*T* vs T^2 curves in the temperature range of 0.4 and 10 K for $BiMnO_3$ (C_p and C_m) and $BiScO_3$ (C_p). The first feature is a large magnetic contribution to the specific heat in $BiMnO_3$ below 10 K which may be originated from a spin-wave contribution. According to the spin-wave theory the specific heat of a ferromagnet will be reduced on applying a magnetic field due to the suppression of the thermal excitations of the spin wave.[31−33] The measurement at 9 T shows a noticeable reduction of the total specific heat as an almost constant shift on the C_p/T vs *T* curves (Figure 5). The almost constant shift retains up to about 60 K (the inset of Figure 4a). This result supports the presence of a spin-wave contribution. The second feature is a low-temperature upturn due to a Mn-hyperfine contribution to the specific heat. This term is caused by the large local magnetic field at the Mn nucleus. Usually this term is represented by AT^{-2}.[31,34] However our data cannot be fit well with this term probably because the hyperfine contribution is difficult to measure correctly by the pulse relaxation method. For this reason, in the fitting, we use the data from 1.5 to 10 K. In this temperature range,

(31) de Jongh, L. J.; Miedema, A. R. *Adv. Phys.* **2001**, *50*, 947.
(32) Okuda, T.; Asamitsu, A.; Tomioka, Y.; Kimura, T.; Taguchi, Y.; Tokura, Y. *Phys. Rev. Lett.* **1998**, *81*, 3203.
(33) Fisher, R. A.; Bouquet, F.; Phillips, N. E.; Franck, J. P.; Zhang, G. W.; Gordon, J. E.; Marcenat, C. *Phys. Rev. B* **2001**, *64*, 134425.
(34) Woodfield, B. F.; Wilson, M. L.; Byers, J. M. *Phys. Rev. Lett.* **1997**, *78*, 3201.

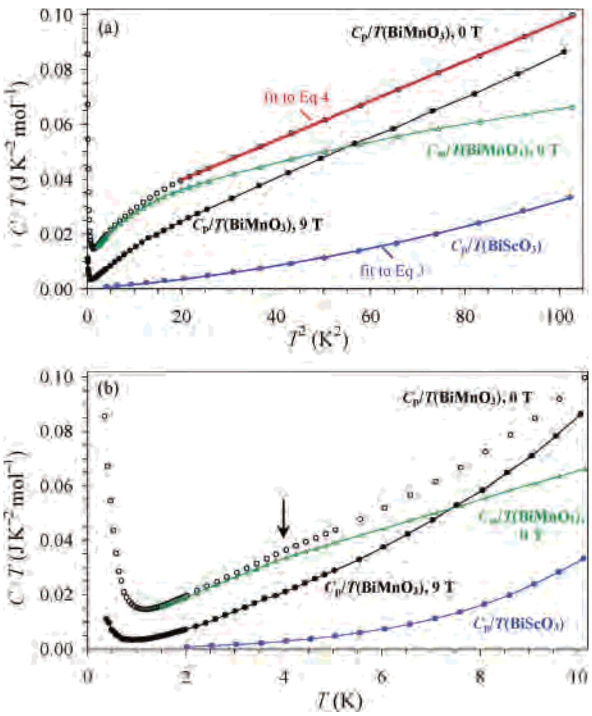

Figure 5. (a) C/T vs T^2 curves between 0.4 and 10 K for $BiMnO_3$ (C_p and C_m) and $BiScO_3$ (C_p). For $BiMnO_3$, the C_p/T curves at 0 and 9 T are given. The solid lines give the fits to eq 3 for $BiScO_3$ and to eq 4 for $BiMnO_3$; other lines are drawn for the eye. (b) C/T vs T curves between 0.4 and 10 K for $BiMnO_3$ and $BiScO_3$. The lines are drawn for the eye. The arrow marks the position of the curvature of the curves.

the data can be measured very accurately by the pulse relaxation method with a PPMS.

Below 10 K, the C_p/T vs T^2 curves of $BiCrO_3$ and $BiScO_3$ are analyzed using the expression

$$C_p = C_l = \beta_1 T^3 + \beta_2 T^5 \tag{3}$$

The fitted parameters are $\beta_1 = 1.36(3) \times 10^{-4}$ J/mol K^4 and $\beta_2 = 1.84(4) \times 10^{-6}$ J/mol K^6 for $BiScO_3$ and $\beta_1 = 1.40(2) \times 10^{-4}$ J/mol K^4 and $\beta_2 = 1.37(2) \times 10^{-6}$ J/mol K^6 for $BiCrO_3$. The Debye temperature ($\Theta_D = (234 N_a N k_B/\beta_1)^{1/3}$, where N_a is the number of atoms per formula unit) of $BiCrO_3$ and $BiScO_3$ obtained from the β_1 coefficient is almost the same (about 410 K). Note that a higher order lattice term proportional to T^5 is needed to fit the data in the temperature range up to 10 K (Figure 5a). This term will strongly affect the fitting results of the low-temperature data of $BiMnO_3$ if one will use the raw C_p data in the fitting procedure instead of the C_m data. The Debye temperature of $BiCrO_3$ and $BiScO_3$ is reasonable. For example, in $La_{1-x}Sr_xMnO_3$ and $La_{1-x}Ca_xMnO_3$, the Debye temperature was reported to be 360−500 K.[29,32−34]

Without the reasonable estimation of the C_l, one could also conclude that there is a large linear term (γ) in the specific heat of $BiMnO_3$ from the C_p/T vs T^2 curve (Figure 5a). Between 4.5 and 10 K, the C_p/T vs T^2 curve is almost linear and can be well fit by the expression

$$C_p = \gamma T + \beta_1 T^3 \tag{4}$$

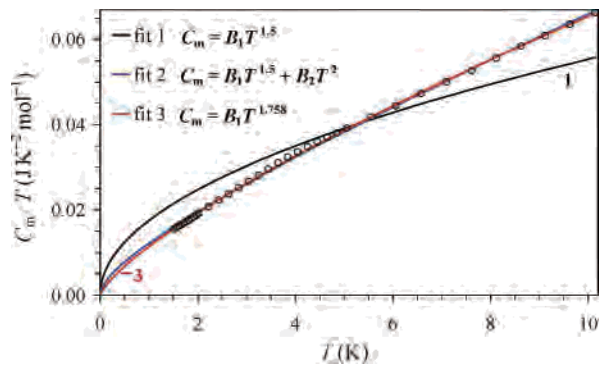

Figure 6. C_m/T vs T curve (circles) at zero magnetic field between 1.5 and 10 K for $BiMnO_3$. The fitting curves by eq 5 with different parameters are given by the lines. The fitting lines are extended below 1.5 K. Fit 4 (not shown) is impossible to distinguish from fit 3 between 1.5 and 10 K on the figure.

with the parameters of $\gamma = 0.025\,31(12)$ J K^{-2} mol^{-1} and $\beta_1 = 7.19(2) \times 10^{-4}$ J K^{-4} mol^{-1}. However, in this case, the Debye temperature is too low (about 240 K) compared with $BiScO_3$. Note that large linear terms in the specific heat were found in a number of insulating manganites.[29,35] However, the detailed explanation for large linear terms has not been put forward in many cases.

The magnetic contribution of a 3D ferromagnet to the specific heat due to spin-waves is usually represented by $B_1T^{3/2}$. However, no simple $B_1T^{3/2}$ term is found in the C_m of $BiMnO_3$ (Figure 6, fit 1). Therefore, the C_m/T vs T curve of $BiMnO_3$ is analyzed using the general equation

$$C_m = B_1 T^{n_1} \exp(-\Delta/k_B T) + B_2 T^{n_2} \tag{5}$$

where Δ is the anisotropy-related spin-wave gap (zero for cubic symmetry)[33] and the second term $B_2T^{n_2}$ reflects some additional contributions to the magnetic specific heat, such as a contribution from spin-glass-like states or the higher terms in series expansions of the magnetic contribution of a 3D ferromagnet.[31] The fitting results are given in Table 1 and Figure 6. A very good agreement between the experimental and calculated C_m/T vs T curves is obtained when we allow to vary n_1 (with $\Delta = 0$ and $B_2 = 0$). However, in this case, the obtained n_1 value of 1.75 does not agree with the simple spin-wave theoretical predictions.[31] Another rather good fit is obtained with $n_1 = 1.5$ when the second term is given by B_2T^2. In all the cases, the introduction of the spin-wave gap improves the fits. The obtained gap does not exceed 1 K. It should be noted that both C_p/T vs T and C_m/T vs T curves of $BiMnO_3$ show the clear curvature near 4 K. It is also interesting to note that the C_m/T vs T curve is almost linear at the temperature ranges of 1.5−4 and 4−10 K (Figures 5b and 6).

Therefore, the specific heat measurements show the presence of the spin-wave contribution at low temperatures. However, the analysis of the data reveals unconventional behavior of the magnetic specific heat, that is, the absence of a simple term $C_m \propto T^{3/2}$. The most reasonable models are

(35) Fritsch, V.; Hemberger, J.; Eremin, M. V.; von Nidda, H. A. K.; Lichtenberg, F.; When, R.; Loidl, A. *Phys. Rev. B* **2002**, *65*, 212405.

Table 1. Fitting Parameters of the Magnetic Specific Heat of $BiMnO_3$ by Eq 5 between 1.5 and 10 K

B_1 (J/(mol K^{n_1+1}))	n_1	Δ/k_B (K)	B_2 (J/(mol K^{n_2+1}))	n_2	R^a	fit^b
0.0175(4)	1.5	0	0	0	1.93×10^{-2}	fit 1
0.0220(2)	1.5	1.02(4)	0	0	9.14×10^{-4}	
0.0081(2)	1.5	0	0.00405(8)	2 (fixed)^c	2.56×10^{-4}	fit 2
0.0118(4)	1.5	0.46(4)	0.00294(11)	2 (fixed)^c	5.07×10^{-5}	fit 4
0.01141(7)	1.758(3)	0	0	0	8.82×10^{-5}	fit 3
0.0126(3)	1.719(10)	0.16(4)	0	0	5.86×10^{-5}	

^{a} $R = \Sigma_{i=1}^{K}(C_m/T(T_i)-C_{fit}/T(T_i))^2/\Sigma_{i=1}^{K}(C_m/T(T_i))^2$, calculated for the C_m/T vs T curve, where K is the number of experimental points. ^{b} See Figure 6. ^{c} The least-squares refinement is unstable when n_2 is varied. Nevertheless, the best fit is obtained for $n_2 = 2$.

given by fits 2 and 4 (Table 1). These models assume the presence of the conventional ferromagnetic spin waves (with a possible small gap) plus contribution from spin-glass-like states. Additional experiments, such as inelastic neutron scattering, will be needed to clarify the behavior of spin waves in $BiMnO_3$ and study the dispersion relation.

In conclusion, the properties of multiferroic $BiMnO_3$ were studied in details by dc and ac magnetization, relaxation, and specific heat. The time- and frequency-dependent magnetic properties were observed indicating the presence of spin-glass-like features below the ferromagnetic Curie temperature of 98 K. Specific heat data revealed the presence of ferromagnetic spin waves.

Acknowledgment. We thank Dr. M. Tachibana of NIMS for valuable discussion.

Supporting Information Available: XRD patterns of $BiMnO_3$, $BiCrO_3$, and $BiScO_3$ (Figures S1), the M vs H curves in the vicinity of the origin (Figure S2), and the comparison of the ZFC dc susceptibilities with the ac susceptibilities (Figure S3) (PDF). This material is available free of charge via the Internet at http://pubs.acs.org.

IC061400B